PNAS
www.pnas.org

Supplementary Information for

Degenerative and Regenerative Pathways Underlying Duchenne Muscular Dystrophy Revealed by Single-nucleus RNA Sequencing

Francesco Chemello, Zhaoning Wang, Hui Li, John R. McAnally, Ning Liu, Rhonda Bassel-Duby, Eric N. Olson

Eric N. Olson, Ph.D.
Email: Eric.Olson@utsouthwestern.edu

This PDF file includes:

Figures S1 to S6
Legends for Datasets S1 to S6

Other supplementary materials for this manuscript include the following:

Datasets S1 to S6

www.pnas.org/cgi/doi/10.1073/pnas.2018391117

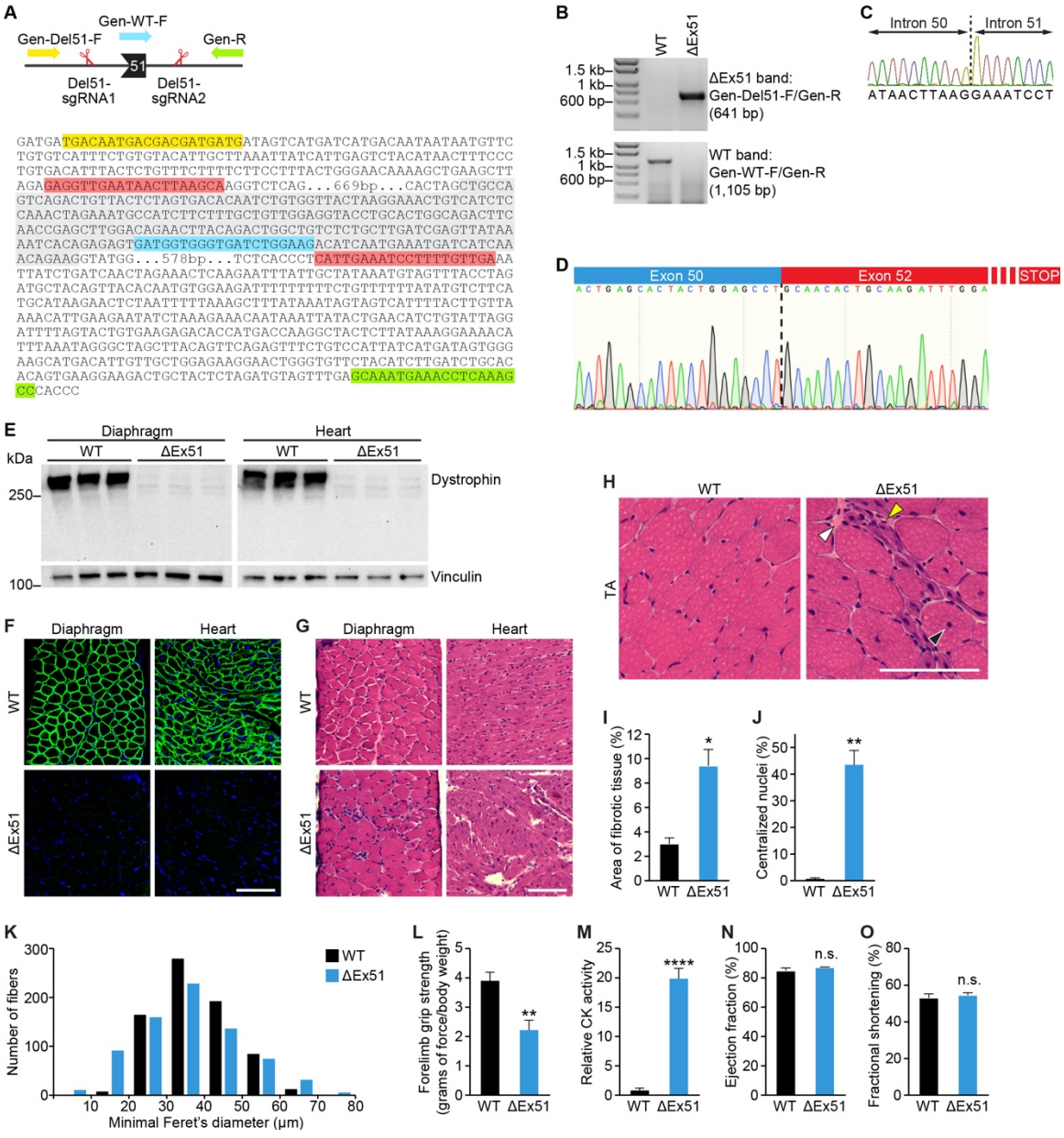

Fig. S1. Generation and characterization of ΔEx51 mice.

(*A* and *B*) Genotyping strategy for ΔEx51 mice. Complementary sequences of the sgRNAs used to remove exon 51 are labelled in red. Primers Gen-Del51-F (yellow) and Gen-R (green) detected the ΔEx51 band in the ΔEx51 but not in the WT mice. Primers Gen-WT-F (blue) and Gen-R (green) detected the WT band in the WT but not in the ΔEx51 mice. (*C*) Sequencing of the ΔEx51 band confirmed the deletion of exon 51 and the formation of a new junction between intron 50 and intron 51. (*D*) Sequencing of RT-PCR products from muscles of ΔEx51 mice confirmed

deletion of exon 51 at RNA level, resulting in the inclusion of 32 novel amino acids prior to the stop codon. (*E*) Western blot analysis showing loss of dystrophin expression in the diaphragm and heart of ΔEx51 mice. Vinculin is the loading control (n = 3). (*F*) Dystrophin staining of the diaphragm and heart of WT and ΔEx51 mice. Dystrophin is shown in green. Nuclei are marked by DAPI stain in blue. Scale bar, 100 μm. (*G*) H&E staining of the diaphragm and heart of WT and ΔEx51 mice. Scale bar, 100 μm. (*H*) H&E images of TA muscle of WT and ΔEx51 mice. White arrow indicates fibrotic tissue, yellow arrow indicates degenerating myofiber, black arrow indicates myofiber central nucleation. Scale bar, 100 μm. (*I*) Quantification of area of fibrotic tissue in whole sections of TA muscles of WT and ΔEx51 mice (n = 3). Data are represented as mean ± SEM. Unpaired Student's t test was performed, $*P < 0.05$. (*J*) Percentage of muscle fibers with centralized nuclei in TA muscles of WT and ΔEx51 mice (n = 3) (1,413 average muscle fibers per muscle). Data are represented as mean ± SEM. Unpaired Student's t test was performed, $**P < 0.01$. (*K*) Size distribution of muscle fibers of TA muscles of WT and ΔEx51 mice. Size was calculated as minimal Feret's diameter. Muscle fibers were grouped in size classes of 10 μm and the number of fibers in each class was plotted (n = 3) (250 muscle fibers per muscle for a total of 750 muscle fibers per condition). (*L*) Forelimb grip strength analysis of WT and ΔEx51 mice (n = 6). Data are represented as mean ± SEM. Unpaired Student's t test was performed, $**P < 0.01$. (*M*) Serum creatine kinase (CK), a marker of muscle damage and membrane leakage, was measured in WT and ΔEx51 mice (n = 6). Data are represented as mean ± SEM. Unpaired Student's t test was performed, $****P < 0.001$. (*N*) Percentage of ejection fraction of hearts of WT and ΔEx51 mice (n = 3). Data are represented as mean ± SEM. Unpaired Student's t test was performed, and no significant difference was observed (n.s.). (*O*) Percentage of fractional shortening of hearts of WT and ΔEx51 mice (n = 3). Data are represented as mean ± SEM. Unpaired Student's t test was performed, and no significant difference was observed (n.s.).

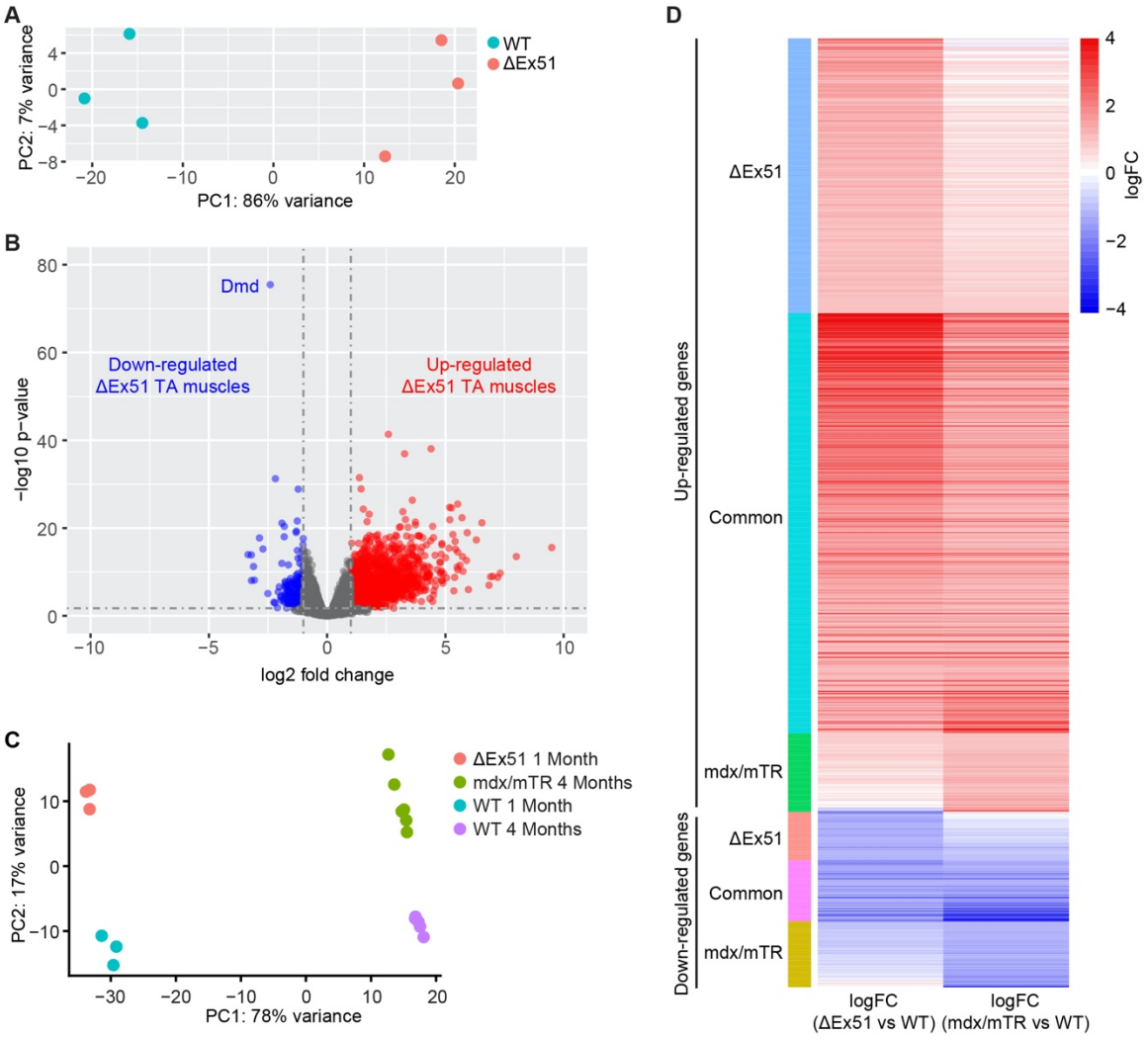

Fig. S2. Comparison of transcriptional changes of muscles of ΔEx51 and mdx/mTR mice.

(*A*) Principal component (PC) analysis of RNA sequencing data of WT and ΔEx51 TA muscles (n = 3). (*B*) Volcano plot showing fold changes in expression and p-values of genes of WT and ΔEx51 TA muscles. The *Dmd* transcript is the most significantly down-regulated. (*C*) Principal component (PC) analysis of RNA sequencing data of TA muscles of 1-month old WT and ΔEx51 mice and of 4-months old WT and mdx/mTR mice. (*D*) Logarithmic fold change (LogFC) of DE genes comparing transcriptome of 1-month old WT and ΔEx51 muscles or 4-months old WT and mdx/mTR muscles. DE genes are grouped according to their significant deregulation in the two analyses.

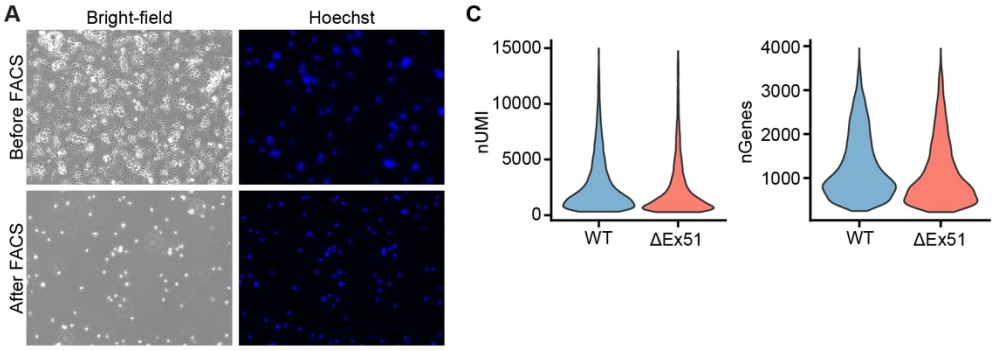

B

Sample	Total number of nuclei	Total number of nuclei after filtering	Mean mapped reads per nucleus	Median genes per nucleus	Sequencing saturation	Reads mapped confidently to genome	Reads mapped confidently to pre-mRNA reference	Reads mapped confidently to introns	Total genes detected
WT TA muscles	7,095	7,013	31,594	1,067	72.5%	86.7%	67.7%	38.1%	23,588
ΔEx51 TA muscles	4,486	4,209	51,422	903	81.1%	80.4%	60.7%	33.1%	23,599

Fig. S3. snRNA-seq analysis of WT and ΔEx51 TA muscles.

(*A*) Preparations of nuclei before and after Fluorescence-activated Cell Sorting (FACS). Nuclei stained with Hoechst dye are shown in blue. Nuclei isolated from myofibrillar debris were used for snRNA-seq. (*B*) Mapping statistics of the sequencing results from each sample. (*C*) Violin plots showing the number of UMI counts (nUMI) and detected genes (nGenes) in each sample.

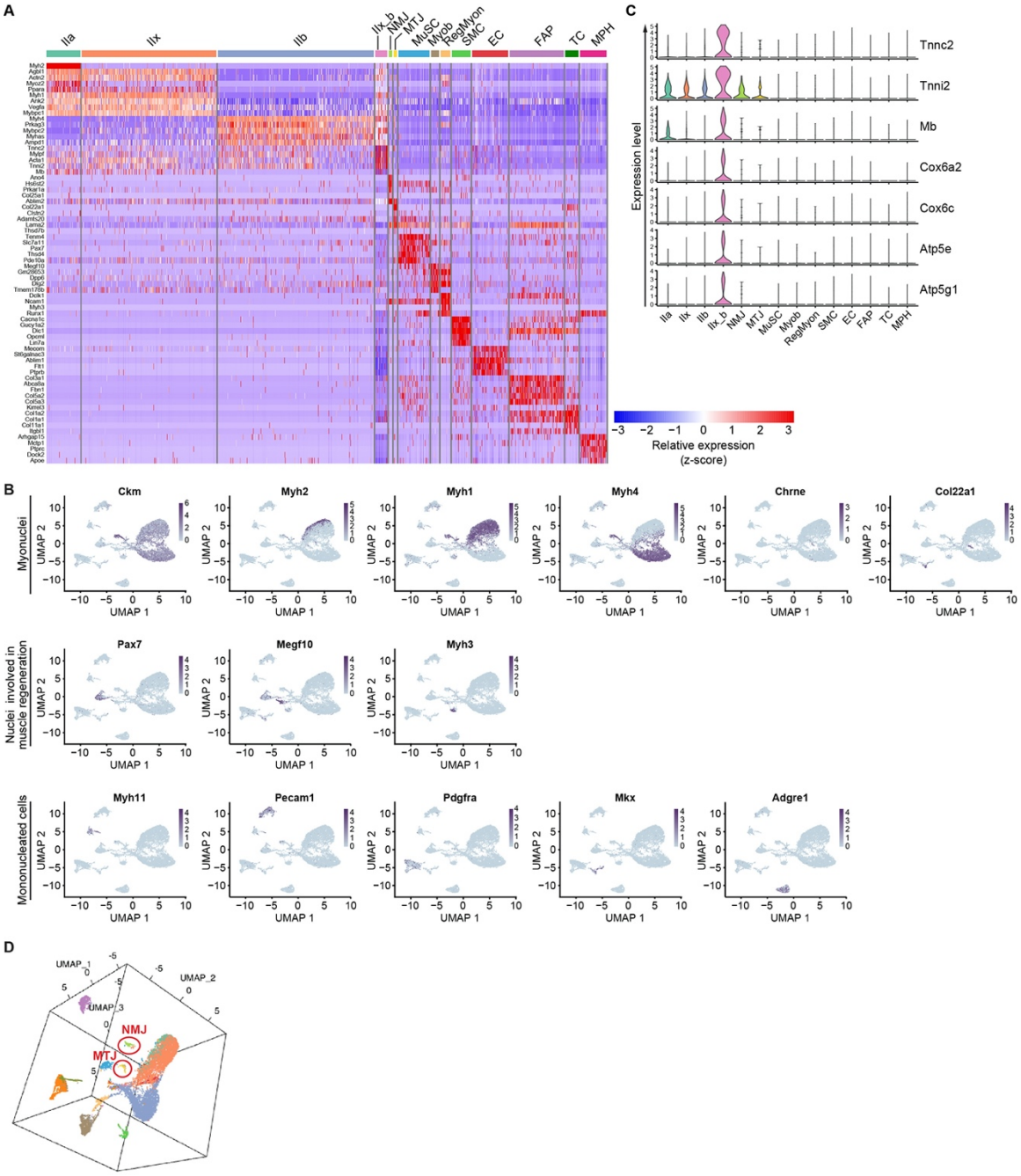

Fig. S4. Transcriptomic characterization of nuclear populations of WT and ΔEx51 TA muscles.

(*A*) Heatmap showing relative expression levels of the top 5 marker genes for each cluster of nuclei. (*B*) UMAPs depicting the expression of the marker genes of each cluster of nuclei. (*C*) Violin plots showing the expression of genes highly expressed in the Cluster IIx_b. (*D*) Three-dimensional UMAP representation of the skeletal muscle snRNA-seq data.

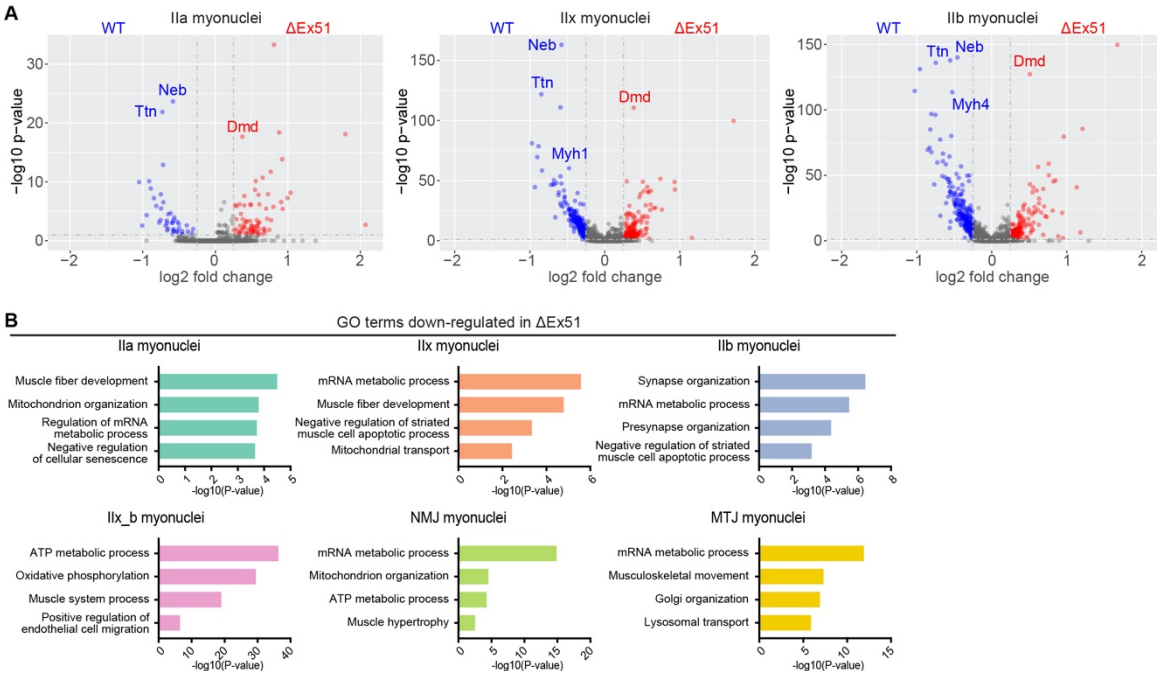

Fig. S5. Changes in gene expression and GO term analysis in ΔEx51 myonuclei compared to WT myonuclei.

(*A*) Volcano plots showing fold changes in gene expression and p-values of genes of IIa, IIx, and IIb myonuclei of WT and ΔEx51 TA muscles. (*B*) Selected top GO terms enriched in down-regulated genes from the different clusters of ΔEx51 myonuclei.

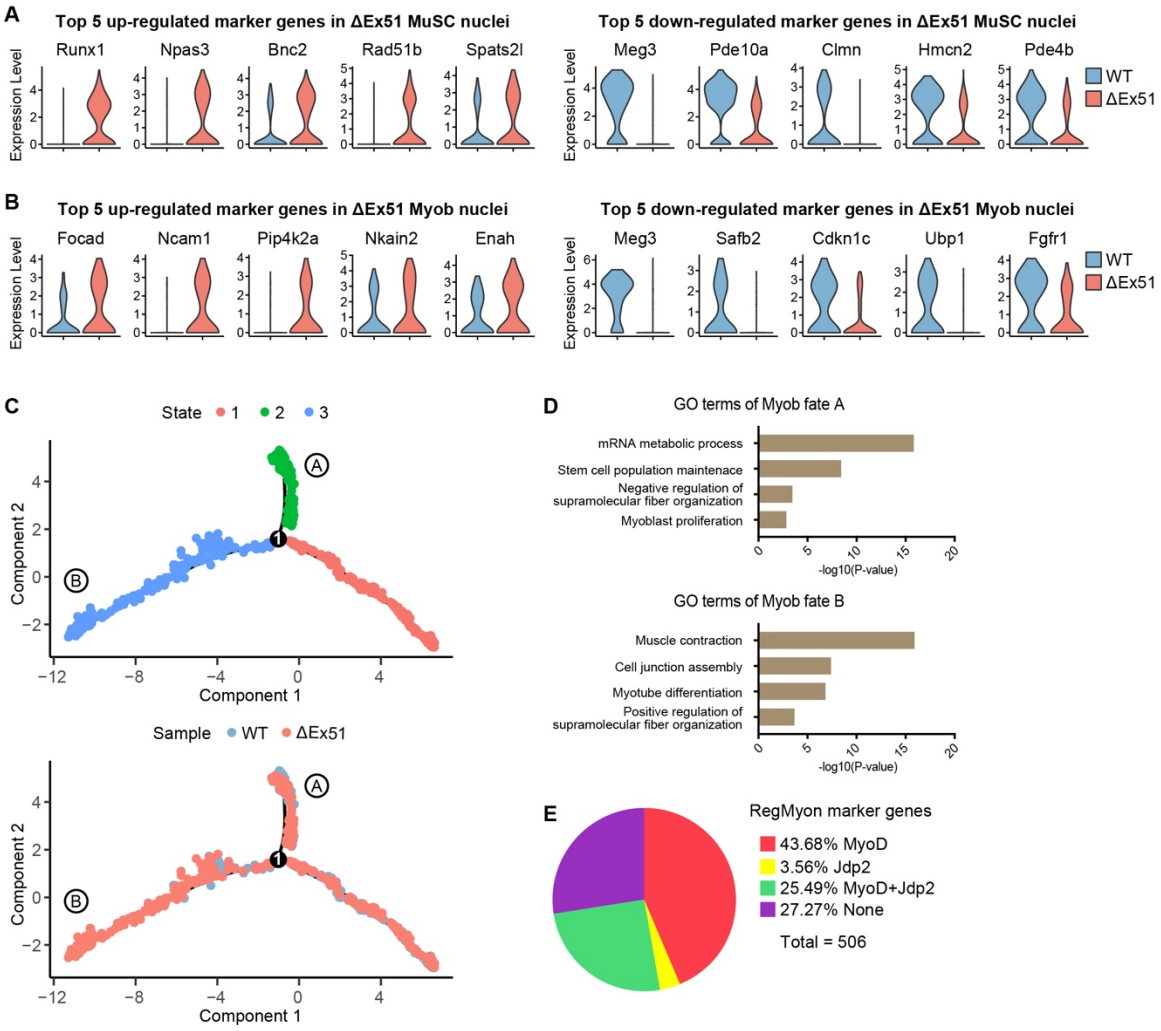

Fig. S6. Identification of specific markers and analysis of gene expression dynamics of WT versus ΔEx51 populations of nuclei involved in regeneration of muscle.

(*A*) Violin plots showing the differential expression of the top up- and down-regulated genes in WT and ΔEx51 MuSC cluster. (*B*) Violin plots showing the differential expression of the top up- and down-regulated genes in WT and ΔEx51 Myob cluster. (*C*) Pseudo-time ordering of all the nuclei of clusters MuSC, Myob, and RegMyon. Each dot represents one nucleus (color coded by cell states (top) or sample origin (bottom)) and each branch represents one cell state. Activation of the MuSC cluster can lead to Myob fate A or to RegMyon fate B, according to Figure 4*C*. (*D*) Selected top GO terms enriched in genes up-regulated in the nuclei of Myob fate A (top), or Myob fate B (bottom). (*E*) Pie-chart showing the

percentages of the RegMyon marker genes with MyoD binding sites associated, Jdp2 motifs in the promoter regions, or both. MyoD binding sites were identified from MyoD ChIP-seq in C2C12 cells. Jdp2 motifs were analyzed using iRegulon.

Dataset S1 (separate file). Differentially expressed genes in ΔEx51 skeletal muscle bulk RNA-seq.

Dataset S2 (separate file). Gene ontology analysis of differentially expressed genes in ΔEx51 skeletal muscle bulk RNA-seq.

Dataset S3 (separate file). Marker genes of nuclear clusters of skeletal muscle.

Dataset S4 (separate file). Differentially expressed genes in ΔEx51 muscle in different types of myonuclei and in different states of Myob.

Dataset S5 (separate file). Gene ontology analysis of differentially expressed genes in ΔEx51 muscle in different types of myonuclei and in different states of Myob.

Dataset S6 (separate file). iRegulon analysis of marker genes of Cluster of RegMyon.